CrossMark

INVITED REVIEW

Tight junctions of the proximal tubule and their channel proteins

Michael Fromm[1] · Jörg Piontek[1] · Rita Rosenthal[1] · Dorothee Günzel[1] ·
Susanne M. Krug[1]

© Springer-Verlag Berlin Heidelberg 2017

Abstract The renal proximal tubule achieves the majority of renal water and solute reabsorption with the help of paracellular channels which lead through the tight junction. The proteins forming such channels in the proximal tubule are claudin-2, claudin-10a, and possibly claudin-17. Claudin-2 forms paracellular channels selective for small cations like Na^+ and K^+. Independently of each other, claudin-10a and claudin-17 form anion-selective channels. The claudins form the paracellular "pore pathway" and are integrated, together with purely sealing claudins and other tight junction proteins, in the belt of tight junction strands surrounding the tubular epithelial cells. In most species, the proximal tubular tight junction consists of only 1–2 (*pars convoluta*) to 3–5 (*pars recta*) horizontal strands. Even so, they seal the tubule very effectively against leak passage of nutrients and larger molecules. Remarkably, claudin-2 channels are also permeable to water so that 20–25% of proximal water absorption may occur paracellularly. Although the exact structure of the claudin-2 channel is still unknown, it is clear that Na^+ and water share the same pore. Already solved claudin crystal structures reveal a characteristic β-sheet, comprising β-strands from both extracellular loops, which is anchored to a left-handed four-transmembrane helix bundle. This allowed homology modeling of channel-forming claudins present in the proximal tubule. The surface of cation- and anion-selective claudins differ in electrostatic potentials in the area of the proposed ion channel, resulting in the opposite charge selectivity of these claudins. Presently, while models of the molecular structure of the claudin-based oligomeric channels have been proposed, its full understanding has only started.

Introduction

About two-thirds of the renally filtered load is reabsorbed in the segments of the proximal tubule. As luminal (primary filtrate) and basolateral (plasma) concentrations are similar for ions and water, this absorption takes place against almost no relevant concentration gradients, but for larger solutes this is different: monosaccharides and amino acids can be absorbed against large gradients until they are virtually absent in the lumen. The transport of ions and water is achieved by sophisticatedly arranged channels, carriers, transporting ATPases in the apical, and basolateral membranes of the epithelial cells. For a multitude of larger molecules, including the abovementioned nutrients, carriers exist in both cell membranes.

A structural prerequisite for any active transport across the epithelial layer to become effective is that immediate back-leakage through the space between the cells is prevented. This is achieved by a sealing structure found in all epithelia, the tight junction (TJ) or *Zonula occludens*. The sealing effect, however, is by far not equal in all epithelia. In epithelia

✉ Michael Fromm
michael.fromm@charite.de

[1] Institut für Klinische Physiologie, Charité—Universitätsmedizin Berlin, Hindenburgdamm 30, 12203 Berlin, Germany

classified as "tight" (e.g., large intestine, renal distal tubules, urinary bladder, and skin), the transcellular pathway is more permeable to ions than the paracellular one through the TJ. In contrast, in "leaky" epithelia (e.g., small intestine, proximal tubules, gallbladder, and capillary endothelia), this is the other way around, meaning that the TJ is more permeable to ions than the cell membranes with their specific transporters [8, 16]. In consequence, leaky epithelia cannot produce or maintain strong ion or osmotic gradients.

For the proximal tubule, this means that luminal concentrations, e.g., for sodium and osmoles (the sum of all solutes) are not significantly reduced during the passage through the proximal tubule. Since in this nephron segment a huge amount of water and solute is reabsorbed, the question is how this can work. The simple answer is that transcellular transport produces an electrochemical gradient which drives ions (and water) through that paracellular path, which by that acts as a "forward leak" enhancing overall reabsorption.

In detail, in the proximal tubule, Na^+ is taken up transcellularly by the Na^+/H^+ antiporter NHE3, the Na^+-glucose symporters SGLT2 and then SGLT1, and several Na^+-amino acid symporters, and basolaterally taken out by the Na^+/K^+-ATPase. The osmotic gradient produced by this transport drives trans- and paracellular water reabsorption. The water transported along this way carries additional Na^+ (classically called "solvent drag"), so that even more water is transported which again carries some ions, and so forth. Since the luminal Cl^- concentration increases along the axis of the proximal tubule, a concentration gradient for Cl^- emerges and drives this anion through the paracellular

pathway too. The resulting lumen-positive potential provides in turn a driving force for further paracellular cation reabsorption. Altogether, this causes the paracellular pathway to boost the transcellular net transport in a dramatic way without consuming excess ATP energy [7].

While the physiological mechanism—as well as the existence of "tight junctions"—were known for decades [21], it much later emerged which molecular fabric provides the tightness and, at the same time, the graded leakiness of the paracellular cleft between the tubular cells [15]. A first step was the identification of the first TJ proteins, "occludin" and several "claudins" [24, 26, 54]. Their names were suggestive for their supposed sealing properties. It was a big surprise when it turned out that some of the claudins arrange in such a way that they form channels for small ions and for water [3, 64]. These channels are distinct from classical channels which perforate the cell membrane, as they lead strictly extracellular through the TJ and are orientated parallel to the lateral cell membranes.

The molecular basis of these paracellular channels is provided by specialized members of the 26-member family of human claudins. Together with the other four-transmembrane-domain (tetraspan) TJ protein family, the three TAMPs (TJ-associated MARVEL proteins) occludin, tricellulin, and marvel-D3, the claudins form typical arrangements of strand meshworks which interconnect the lateral cell membranes of neighboring epithelial cells (Fig. 1a). By this, they are capable to form a general seal against unlimited passage of solutes and water through the epithelial wall [54, 77] but simultaneously form a pathway for paracellular transport
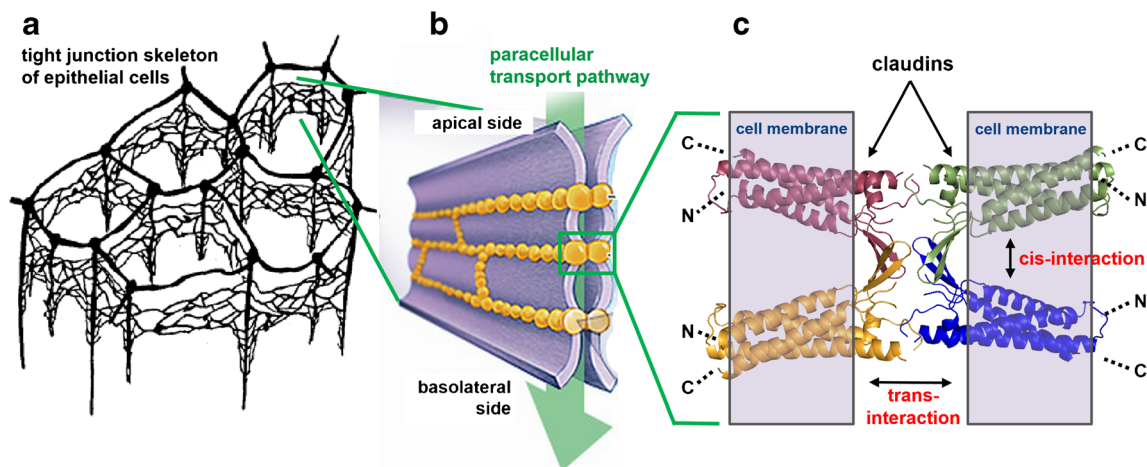
Fig. 1 Tight junction (TJ) skeleton, paracellular pathway, and arrangement of claudins. **a** Strand meshwork of the bicellular and tricellular TJ. Cells were omitted so that the skeleton of TJ strands remains. Taken with permission of the publisher from [48]. **b** Magnified detail showing strands of TJ proteins. In the presence of channel-forming TJ proteins, paracellular transport driven by electrochemical gradients takes place. **c** Magnified detail showing strand formation by claudins of two adjacent lateral cells (scheme is based on a claudin-15 polymer model [79]). Claudins consist of two extracellular loops, four transmembrane regions, and a short intracellular loop and N- and C-terminals. They either form pure barriers or paracellular channels for cations, anions, or water. TJ proteins interact with each other within the same cell membrane (cis-interaction) and across neighboring cell membranes (trans-interaction)

(Fig. 1b). All of these tetraspan TJ proteins, including all claudins (Fig. 1c), feature two extracellular loops. Their contribution to formation of TJ strands depends on *cis*-interaction (within one membrane) and *trans*-interaction (between opposing plasma membranes) between the single proteins [59]. Most epithelial cells express an assortment of different claudins forming mainly heteropolymeric TJ strands [27, 58]. However, not all claudins are compatible with each other. For instance, claudin-1 interacts in *trans* with claudin-3 but not with claudin-2 while claudin-16 and claudin-19 interact in *cis* but not in *trans* (for overview [31]). For the claudins expressed in the proximal tubule, the pattern of compatibility is not investigated so far.

As mentioned above, the paracellular channels are not crossing membranes, as transmembranal channels do but are oriented parallel to the lateral membranes allowing permeation through the TJ. They are formed by the extracellular loops of TJ proteins interacting with extracellular loops of TJ proteins located in the opposing cell membrane. To present knowledge, channel-forming claudins are selective either for small cations or for small anions, and in at least one case also for water [43].

Tight junction proteins of the proximal tubule

TJ proteins described to be present in the proximal tubule [36, 37] are claudin-2 [20, 37], claudin-10a [30, 83], claudin-11 [19, 37], and claudin-17 [42], and the TAMPs occludin [33] and tricellulin [34].

What one may miss in that list is claudin-1, as this pure barrier former is present in many other epithelia. On mRNA level, claudin-1 and also claudin-12 were detected in proximal tubules [1, 11]. However, there is no study so far claiming their presence on protein level. Thus, it may be rather questionable whether claudin-1 is involved in tightening the proximal tubule.

In conclusion, all but one of the claudins identified in the proximal tubule are channel formers, namely claudins 2, claudin-10a, and claudin-17 [31], and only claudin-11, occludin, and tricellulin function as sole barrier formers [29].

Cation-selective paracellular channels

Claudin-2 is typically expressed in all leaky epithelia of the body, including the proximal tubule. Using Madin-Darby Canine Kidney (MDCK) type I cells, a "tight" renal tubular cell subclone naturally devoid of claudin-2, it was shown that introducing claudin-2 into these cells converted them from high- to low-resistance cells [25]. The channel properties of claudin-2 were then discovered in a cell line analogous to MDCK I, MDCK C7, where the Na^+ conductivity of the cell layer was 0.2 mS/cm^2 in vector controls, but when transfected with claudin-2, it reached 1.7 mS/cm^2. The Cl^- conductivity was 0.2 mS/cm^2 in both cell lines, and the permeability for mannitol, lactulose, and 4 kDa-dextran was unchanged.

Thus, claudin-2 forms paracellular channels selective for small cations like Na^+ and K^+ but seals against the passage of anions and larger solutes [3]. This feature proved to be of paramount importance for the proximal tubule explaining its leakiness. After all, claudin-2 represents the long sought-after molecular component for paracellular cation reabsorption.

Several years later, it was found that the same claudin-based channel is also permeable to water [64]. This feature is detailed in a following chapter on paracellular water transport.

Claudin-15 is a major paracellular ion channel former which, however, is not present in the kidney. Being functionally comparabtle to claudin-2, it constitutes cation-selective channels. It was the first claudin of which a crystal structure was solved [78]. From this information, molecular channel models for this and other claudins have been derived (Fig. 1c) [14, 79]. These models are detailed in the final chapter of this review.

Claudin-10 is expressed throughout the entire kidney tubule; however, it exists in at least two functionally relevant splice variants [30, 83] which exhibit distinct localization and function, claudin-10a and claudin-10b. Local discrimination is not easy, because isoform-specific antibodies discriminating between the a and b variant are lacking. Thus, distinction between claudin-10a and claudin-10b was achieved by RTPCR or in situ hybridization so far [30, 83].

Claudin-10b is expressed in many epithelia, unlike claudin-10a which is specific for the kidney and uterus [30]. Like claudin-2 and claudin-15, it forms paracellular cation channels [30, 83]. Its functionally most important site is the thick ascending limb of Henle's loop (TALH), where it acts in spatial neighborhood with two other claudins involved in the reabsorption of divalent cations, claudin-16 and claudin-19 [50]. It is emphasized here because of its kinship to claudin-10a (see below).

Anion-selective paracellular channels

The proximal tubule is also the main nephron site of Cl^- reabsorption. A major part of that transport is paracellular and passively driven by the lumen-negative transepithelial voltage in the early proximal tubule and the outwardly directed concentration gradient for Cl^- in the later proximal tubule [6]. Therefore, one would expect anion-selective channel-forming TJ proteins in the proximal tubule. Indeed, two claudins were identified so far to possess this feature, claudin-10a and claudin-17.

Claudin-10a deviates from claudin-10b only in its first transmembrane segment and first extracellular segment [49, 83]. As a result, it differs in charge selectivity from claudin-10b and represents one of the two major anion channels of the TJ. It is localized mainly in the proximal tubule.

Claudin-17 was not analyzed functionally until 2012, where evidence was presented that it forms anion-selective channels [14, 42]. Unlike claudin-10a, it is permeable also for HCO_3^-. Claudin-17 protein expression is abundant in the renal cell lines LLC-PK1, MDCK II, and MDCK C11, all of which are generally used as epithelial cell models for the proximal tubule. Immune-fluorescence indicated its presence also in kidney tubules where it appears to gradually decrease from proximal towards distal segments [42]. Other localizations known so far are brain capillaries [42], hair follicles [9], and breast epithelium [80].

Claudin-10a and claudin-17 seem to have similar functions, as both are able to contribute to absorption of anions. Thus, both appear to represent the molecular correlate of the high Cl^- permeability of the proximal nephron. Neither regulation nor function of both claudins has been elucidated so far in vivo.

In general, the paracellular pathway of the proximal tubule is not cation- or anion-selective as a whole but consists of independent, parallel pathways for cations (claudin-2) and anions (claudin-10a, possibly claudin-17). It is unknown so far, whether cation- and anion-selective claudins are arbitrarily intermixed, or arranged in a mosaic-like pattern as observed in the TALH for claudins of different functions [50].

Tight junction freeze-fracture electron microscopy and sites of pore and leak pathways

The ultrastructure of TJs can be analyzed by electron microscopy (EM). In ultra-thin sections, the TJ contacts of neighboring cells appear to fuse the membranes and can be seen as so-called "kissing points" [16]. However, these give only little information about the TJ itself.

With freeze-fracture EM (FFEM), the TJ strand network can be visualized and further analyzed in respect to various parameters that may be connected to the barrier properties of the TJ [74, 76]. First of all, the TJ appears as a net-like meshwork of several strands or only one single strand. The number of strands in the tight junction meshwork can vary considerable between epithelia, and it has been shown that this number indeed has a logarithmic relation to transepithelial resistance (TER) [12, 13, 46]. However, this relation does not allow comparison of different epithelia [47], but in general, in leaky regions of tissues, the number of strands is often lower than in tighter tissue regions.

Besides variations in different species, it has been demonstrated that in the proximal tubule 1–2-stranded TJs are present in the *pars convoluta* (segments S1 and S2) (Fig. 2a) and 3–5 strands in the *pars recta* (segment S3) [62] (Fig. 2b). Besides strand number also the depth of the total TJ network appears to correlate with the denseness of the barrier, the distance between single strands increases with increasing tightness [62]. However, even in the S3 segment, the strand spacing is narrow, possessing a network depth of around 100 nm [62].

As by fracturing, the cell membranes are split into halves, association of TJ strands or particles with one or the other membrane leaflet can also be used to gain information about the functional state of the barrier. The protoplasmatic fracture face (P-face) is associated with the protoplasm and is viewed from outside the cell. The cytoplasm is behind that fracture plane [10]. The second plane, the exoplasmic fracture face (E-face) is associated with the extracellular space and is viewed from inside the cells. The P-face usually reveals particles and strands, while the E-face usually reveals the corresponding grooves, when standard fixation with aldehydes is performed [60, 75]. Evaluation and

Fig. 2 Freeze-fracture electron micrographs of proximal tubule TJs. **a** *Pars convoluta* and **b** *pars recta* of the proximal tubule of the dog kidney. While in this species, the *pars convoluta*, the TJ consists of one continuous strand, there are 4.6 ± 1.6 (mean ± SD) particle-type strands in the *pars recta* with a total mesh extension of about 100–150 nm. Magnification 60,000×. BB denotes brush-border (microvilli). *Arrowheads* indicate the direction of shadowing. Image taken with permission of the publisher from [62]
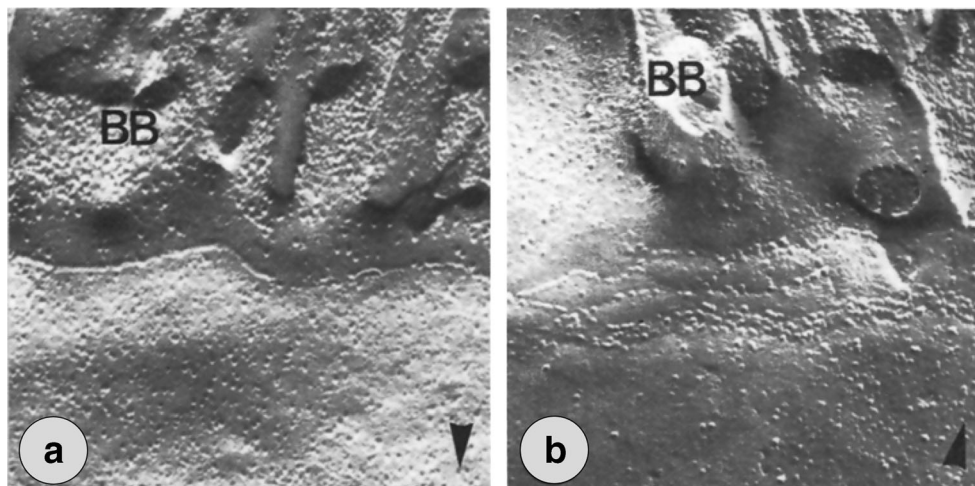
comparison of the ratios between E- and P-face associations may indicate changes in interaction of TJ proteins with each other or with TJ - associated proteins that link it to the cytoskeleton. Different compositions of TJ proteins have been shown to shift the ratio of P- to E-face association and also to affect the TJ barrier [45, 58, 86]. For example, claudin-2 as a predominant claudin of the proximal tubule may shift the usual ratio from P- towards E-face association [24]. However, the TJ of the proximal tubule consists of several TJ proteins and possesses mainly P-face associated TJs [68].

Another feature besides strand number and face association is the form of the meshwork lines: they vary between rectangular and largely parallel or round and curvy. While in most TJs, the strands form rectangular meshes, round and curvy appearance is connected to predominant presence of claudin-3 or claudin-4 [27, 51, 81]. Furthermore, there are two distinctive patterns of TJ strands. The "continuous type" consists of smooth and uninterrupted strands. The other pattern, "particle type", is bead-like and appears as a dotted line formed by particles. The linear, continuous strands are assumed to form tighter barriers than strands which have a particle-type appearance. However, the endothelial TJ strands of the very tight blood brain barrier are also of the particle type. Thus, it is still not known whether the particle-type TJs possess functional relevance or only indicate presence of specific TJ proteins, as especially for claudin-2, that forms paracellular channels for cations [3] and water [64], a connection to particle-type strand appearance has been observed [25, 63]. Also in the claudin-2-expressing proximal tubule, particle-type strand appearance can be found [13]. However, one also could assume that this rather might reflect specific interactions than presence of claudin-2 alone, as the introduction of claudin-2 not necessarily leads to the appearance of particle-type TJs [64].

Parameters as complexity and continuousness also do not necessarily mean a tight TJ barrier, as for example, a lack of the channel-forming claudin-2 and claudin-15 in a double-knockout lead to a less complex and discontinuous strand network in the intestine, although the transepithelial conductance decreased [84]. However, the depth of the total TJ network was increased [84].

Discontinuities and breaks in TJ strands, which can be seen in FFEM, are discussed to represent a weak TJ network and to allow passage of solutes, as paracellular passage is differentiated into two different pathways: when permeabilities for small and large solutes were determined using a spectrum of differently sized polyethylene glycols (PEG) and observing different effects of EGTA or caprate-treatment, it became obvious that restrictive pores (radius 0.43–0.45 nm) and nonrestrictive pores are present [85]. For the proximal tubule, calculations that supported this finding discriminated these pathways into pores and slits [32]. Later the two pathways were

named "pore pathway" and "leak pathway" [72, 82] and are assumed to be regulated by different components of the TJ.

The "pore pathway" is undisputedly specified by the expression of channel-forming claudins and has a charge- and size-restrictive cutoff ion radius of ~4 Å [82]. In the proximal tubule, the earlier calculations found this pathway to cover 91% of NaCl permeability [32], fitting well to the high expression levels of channel-forming claudins like claudin-2 within the proximal tubule.

For the size-selective, second class of paracellular passage, the term "leak pathway" has been introduced. It ranges between 4 and 40 Å [15] and is comparatively rare, occupying 0.04% of the total TJ length in the proximal tubule [32]. As structural correlate of the "leak pathway," two assumptions are discussed. One comprises a step-wise passage of macromolecules through reversible and coincidental strand breaks within the TJ network, as they can be found in FFEM [4, 72, 82]. The other additionally discusses the tricellular TJ, which is formed at the TJ contact region of three cells, as this area is supposed to be involved in macromolecule passage [40, 41]. Tricellulin, which is mainly present within the tricellular TJ [34], is a regulator of the "leak pathway" here [22]. Due to its dimensions, the "leaks" are not only offering a route for paracellular passage for large solutes but also for ions. In leaky epithelia like the proximal tubule, the contribution of the "leak pathway" to ion conductance is low and can be neglected, as paracellular conductance is mainly determined by channel-forming claudins like claudin-2 [39].

Physiological role of paracellular water permeability

The identification of claudin-2 as a cation [3] and water [64] channel has provided the molecular basis for the paracellular Na^+ and water movement in the proximal tubule. These in vitro studies using overexpression systems have been confirmed by studies on claudin-2-deficient mice [55, 70]. Muto and coworkers analyzed the role of claudin-2 in paracellular permeability properties of renal proximal tubules. Studies on morphology of wild-type and claudin-2-deficient proximal tubule revealed (i) no significant differences in ultrathin section electron microscopy, (ii) no differences in the number of kissing points (one or two), where plasma membranes of neighboring cells made complete contact, (iii) no differences in the number of TJ strands, only one or two TJ strands as shown by freeze-fracture replica electron microscopy.

In contrast to the morphology, functional studies revealed strong differences between wild-type and claudin-2-deficient kidneys [55, 70]. The net transepithelial reabsorption of Na^+, Cl^-, and water in isolated, perfused S2 segments of

claudin-2-deficient proximal tubules was decreased by about 38, 24, and 28%, respectively, compared to wild-type tubules. It was shown that the decreased Cl⁻ reabsorption in the absence of claudin-2 was due to the reduction of paracellular Na⁺ reabsorption, since Cl⁻ accompanies Na⁺ for electroneutrality reasons through the anion-selective claudins 10a and/or 17. Thus, although being a cation channel, claudin-2 mediates the NaCl reabsorption in proximal tubules of the kidney. This results in an osmotically driven transepithelial water reabsorption. For this, aquaporin 1 as the molecular basis of the transcellular pathway was uncovered in the 1990s [2]. The contribution, or even existence, of a specific paracellular water pathway has been controversially discussed for decades, although studies on aquaporin 1 knockout mice had shown a reduction of proximal tubule net water reabsorption by only 50% and thus suggested the existence of an aquaporin 1-independent pathways of water reabsorption [69]. With the finding that claudin-2 permits the passage of water through its pore [64], the molecular structure of the paracellular water pathway was uncovered.

Similar findings as shown by Muto et al. were obtained by Schnermann and coworkers, who showed a reduction of fractional proximal fluid reabsorption in claudin-2-deficient mice by 23.5% [55, 70]. The somewhat lower estimate of claudin-2-dependent proximal fluid reabsorption may be due to the fact that Schnermann investigated S1 segments, whereas the study of Muto was performed on S2 segments, and it was shown that claudin-2 expression in the proximal tubule increases along its axis with lower levels in S1 than in S2 and S3 segments [20, 37].

If one disregards all previous evidence for claudin-2-mediated water transport, the findings on claudin-2-deficient mice would also be consistent with claudin-2-mediated Na⁺ reabsorption, creating an osmotic gradient for water movement along the transcellular pathway through aquaporin 1 channels. However, this possibility could be excluded due to the findings in cell culture studies [63, 64]. It has been shown that the Na⁺ and water passage through claudin-2 are coupled, and both share the same pore since (i) claudin-2-mediated water movement could be induced by a gradient for NaCl in the absence of any osmotic gradient, (ii) osmotically induced water movement caused net paracellular Na⁺ transport in claudin-2-expressing cell layers [64], (iii) the mutation, which reduces Na⁺ permeability of claudin-2, concomitantly reduces water flux, and (iv) blocking of the claudin-2 pore reduces Na⁺ and water permeability [63].

The claudin-2 pore is well described by Yu and coworkers [5, 44, 87]. It has a diameter of about 6.5 Å; thus, water molecules with a diameter of 2.8 Å and dehydrated or partially dehydrated ions (Na⁺, K⁺, Ca²⁺) can pass that pore (Fig. 3). Different amino acid

residues (aa) in the first ECL, which line the narrowest part of the pore, were identified to be D65, I66, and S68. Charge neutralization of the negative aa D65 resulted in a decreased Na⁺ and water permeability, and other interventions which inhibit Na⁺ permeability were associated with decreased water permeability [63].

The reduced reabsorption of Na⁺, K⁺, and Cl⁻ in proximal tubule of claudin-2-deficient mice seems to be completely compensated in more distal tubule segments, as indicated by the unchanged fractional excretion (FE) of these ions [55, 70]. This finding is consistent with results on claudin-2-null mice obtained by Yu and coworkers, who found no differences in urine Na⁺ concentration between claudin-2-null and wild-type mice [56]. An increased activity of the Na-K-2Cl cotransporter in the thick ascending limb of Henle's loop is the primary mechanism for compensation of reduced Na⁺ reabsorption in proximal tubule [56]. In contrast, the missing paracellular water reabsorption in proximal tubule cannot be compensated in more distal segments, as shown by the increased urine volume and decreased urine osmolality in the absence of claudin-2 [55, 70].

Additionally to the NaCl and water reabsorption, claudin-2 is involved in Ca²⁺ reabsorption in the proximal tubule [23]. The fractional excretion of Ca²⁺ is greater in claudin-2-
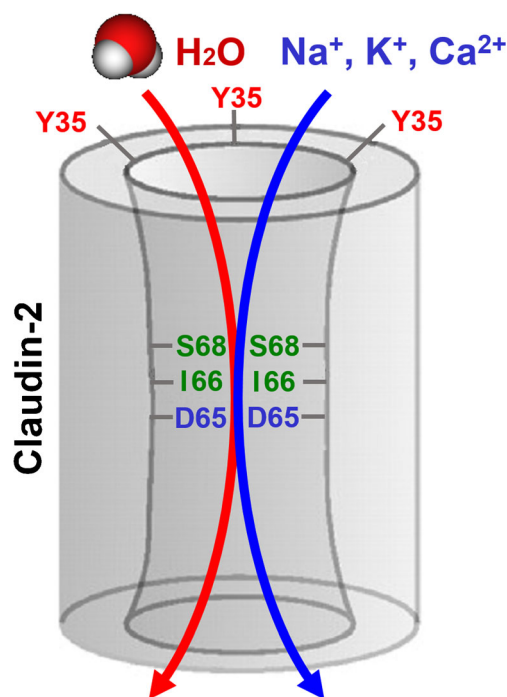

Fig. 3 Model of the claudin-2 pore. The claudin-2 pore with a diameter of about 6.5 Å allows the passage of water molecules with a diameter of 2.8 Å and of dehydrated or partially dehydrated ions (Na⁺, K⁺, Ca²⁺). Different amino acid residues in the first ECL, which line the narrowest part of the pore, were identified to be D65, I66, and S68. Neutralization of the negatively charged D65 (D65N) resulted in a decreased Na⁺ and water permeability [63]. Taken with permission of the publisher from [5] modified

deficient mice compared to control mice [55, 70]. In proximal tubule, a large fraction of Ca^{2+} is reabsorbed by the paracellular route [17, 71], and it has been shown that the claudin-2 pore is permeable to Ca^{2+}, with an approximately fourfold lower permeability than to Na^+ [87]. Thus, the increased FE of Ca^{2+} in claudin-2-deficient mice results from impaired paracellular Ca^{2+} reabsorption in the proximal tubule mediated by claudin-2.

A recent study concerning the role of paracellular Na^+ reabsorption in proximal tubule revealed that this transport is required for efficient utilization of oxygen in the service of

Na^+ transport in the kidney [56]. This study compared the whole-kidney Na^+ reabsorption and oxygen consumption in anesthetized wild-type and claudin-2-deficient mice and found no difference in Na^+ reabsorption, whereas oxygen consumption was 80% higher in KO mice; thus, the efficiency of O_2 utilization for renal Na^+ transport was much lower in the absence of claudin-2. The oxygen consumption was increased in the outer medulla and unchanged in the cortex, and it was due to an increased activity of the $Na^+K^+2Cl^-$ symporter, which compensates for the reduced Na^+ reabsorption.

In summary, the claudin-2 reabsorption in proximal tubule induces an efficient NaCl uptake and water reabsorption.
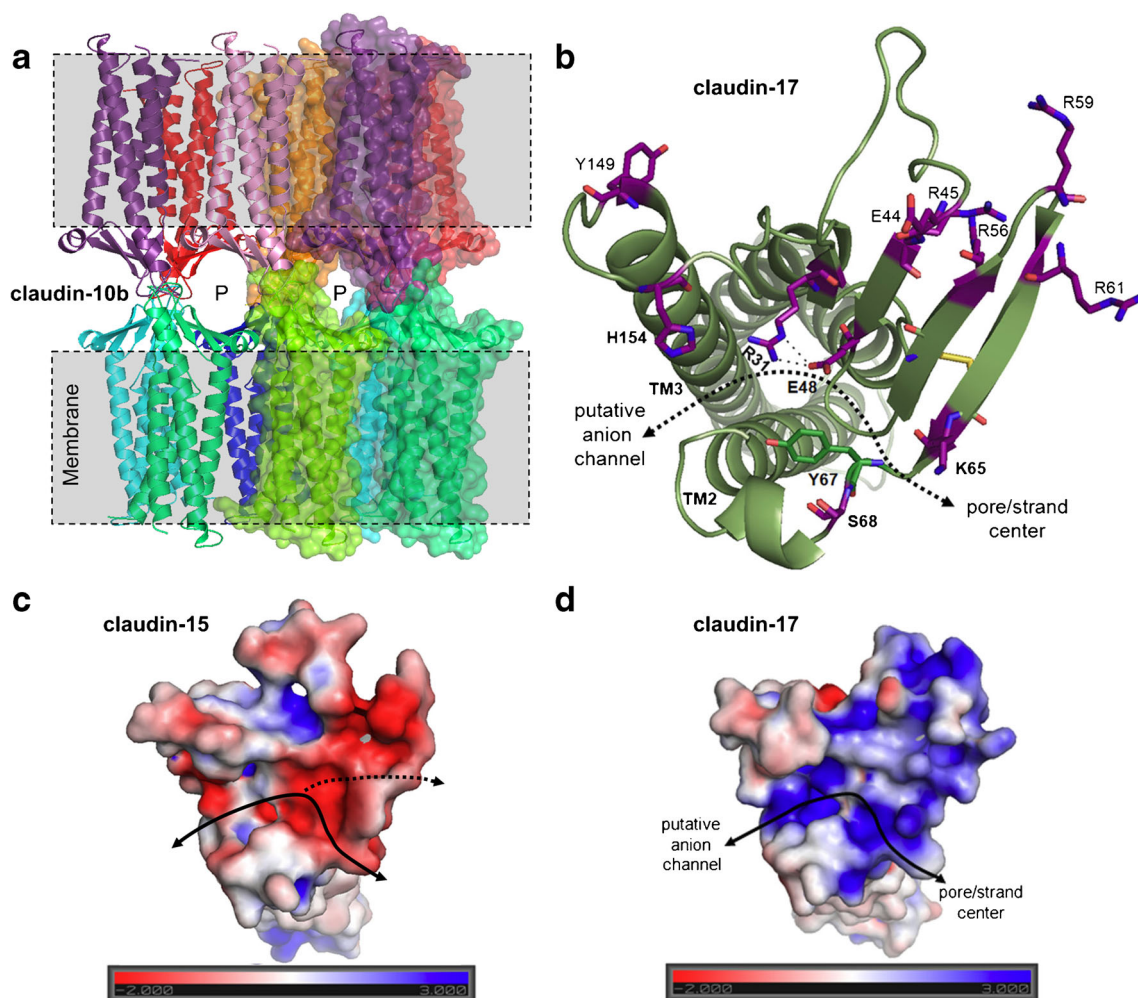
Fig. 4 **a** Potential TJ strand architecture of a cation-selective channel former is shown for claudin-10b (instead of claudin-2, the cation channel-former of the proximal tubule). Claudin-2 was not modeled so far, because for that a high homology with claudin-15 is advantageous, which claudin-10b indeed has. The potential strand architecture was obtained by aligning caudin-10b [52] to the claudin-15 polymer model suggested by Suzuki et al. [79]. Individual claudin protomers are shown in *different colors on the left side* with backbone as cartoon and on the *right side with overlaid surface*. Plasma membranes are depicted as *gray boxes*, and the proposed ion pore is marked "P". The model was taken from [52]. **b** Homology model of claudin-17 protomer based on claudin-15 template (PDB 4P79), view from the extracellular side, backbone as cartoon, residues analyzed as sticks in magenta. Highlighted is the part (*dotted double arrow*) proposed to line the pore within the anion channel formed by a claudin-17 oligomer. **c** and **d** Differing electrostatic potentials (units kT/e) on the surface of claudin-15 and claudin-17 protomers in the area of the proposed pore (*double arrow*) are in line with the opposite charge selectivity of claudin-15 and claudin-17 ion channels, respectively. The *dotted arrow* in **c** indicates a variant course as suggested by Suzuki et al. [79] and by Fig. 4a. Parts **b**, **c**, and **d** taken with permission of the publisher from [14]

Additionally, the paracellular Na$^+$ reabsorption in proximal tubule ensures an efficient oxygen utilization in the kidney.

Molecular models of claudin-based channels

Recently, crystal structures of claudin-15, claudin-19, and claudin-4 revealed their 3D structure with a characteristic β-sheet comprising β-strands 1–4 from ECL1 and β-strand 5 from ECL2, which is anchored to a left-handed four transmembrane helix bundle [67, 73, 78]. This allowed detailed homology modeling of other claudins including claudin-2 [38], claudin -10a, claudin-10b [52], and claudin-17 [14].

A first model of TJ strand architecture proposed for the channel-forming claudin-15 consists of an antiparallel double row cis-arrangement of claudin-15 protomers (structural units) [79]. In addition, interaction data for claudin-1, claudin-3, and claudin-5 were found to be at least partly compatible with an antiparallel double row arrangement [53, 57]. The strand model contains two different cis-interfaces per tetrameric unit: one interface leads to linear arrangement of claudin protomers in the claudin-15 crystal packing [78] and is formed between an ECL2 motif (F, Y/F, x(9–10),E, L/I/M/F) conserved among classic claudins [38] and residues of the small extracellular helix (ECH) in the ECL1 [78]. However, whether this interface is part of native TJ strands is unclear. The second suggested cis-interface supported by crosslinking data [5, 79] is formed through antiparallel interactions between two β4-strands of ECL1 forming an extended β-sheet [79].

Other claudin arrangements are conceivable, too. For instance, experimental data for claudin-3, claudin-5, claudin-16, and claudin-19 [28, 65] and in silico multiscale course grain molecular dynamics simulations for claudin-5 [35] indicated also other dimer interfaces comprising transmembrane helices. Recently, a symmetric cis-tetrameric unit of claudin strands was suggested. Here, the 1st interface is based on a modification of the cis-interface found in the claudin-15 crystal packing and a second interface contains a large contact surface involving transmembrane helices two and three [57].

In the model of claudin-15 TJ strands, Suzuki et al. suggested that two cis-double rows are joined in trans between opposing cells forming a β-barrel-like structure of the ion pore [79]. While providing very useful ideas of a potential TJ architecture (Fig. 4a), this model is limited by steric and functional challenges for channel-forming (claudin-2, claudin-10, claudin-15; [38, 52]) and barrier-forming claudins like claudin-3 [57].

ECL1-residues affecting paracellular permeability for solutes identified by site-directed mutagenesis were reviewed previously [38]. For instance, D65 in claudin-2 [87] and the corresponding positions in claudin-10a (R62) [83] and claudin-17 (K65) [14, 42]

were identified as a key determinant for charge selectivity of the channels. For structural comparison, the ECL1-residues from different claudins were mapped onto the ECL1 structure of claudin-15. The mapping showed that residues-affecting permeability and hence suggested to line the ion pore are located on both sides of the ECL β-sheet [38]. In contrast, the polymeric channel model suggested by Suzuki et al. [30] predicts only one side of the β-sheet to line the pore. Thus, it remained unclear whether both sides of the β-sheet contribute directly to the pore lining.

A detailed structure-function analysis of claudin-17 was performed by analyzing the impact of charge-reversing or charge-neutralizing mutations on anion permeability. K65 (corresponding to charge selectivity filter in claudin-2) was found to be involved more strongly in charge-selective ion permeation than other positively charged residues in the ECL1 (R45, R56, R59, R61). In addition to the positive charge, the shape and H-bonding capability of K65 were found to be necessary for the formation of an anion-selective ion channel. Furthermore, position 68 of claudin-17 was shown to be involved in formation of an anion-selective channel [14].

To gain structural insight into the anion channel formed by claudin-17 and to explain the experimental findings, homology modeling of claudin-17 using claudin-15 and claudin-19 as templates was performed (Fig. 4b). The claudin-17 model [14] indicated a folding very similar to that of other classic claudins [18, 61, 66, 67, 73, 78] including a left-handed four-transmembrane helix bundle and an extracellular β-sheet. However, slight differences within the helix bundle, ECL1 and ECL2, were suggested.

Modeling and the functional data indicated a hydrophilic furrow in the center of the extracellular part of the claudin-17 protomer to line the anion pore which is likely to be formed by an oligomeric claudin channel at cell-cell contacts. The furrow spans from a gap between the extracellular ends of transmembrane helices two and three along R31, E48, and N53 to a gap between K65 and S68 (Fig. 4b). For other channel-forming claudins, ions could potentially pass through a similar furrow. This idea is underlined by the differing electrostatic potentials on the surface of the corresponding furrows of claudin-2, claudin-10b, claudin-15 versus that of claudin-10a and claudin-17 fitting to the opposite charge selectivity of the respective channel (Fig. 4c, d) [14, 78].

Based on the finding that K65R or S68E in claudin-17 impeded ion permeability and modeling, it was proposed that a lack of electrostatic interaction between these positions might contribute to pore formation [14]. Consistent with this idea, such a pore blocking interaction is conceivable for barrier-forming claudins

(claudin-1, claudin-3 to claudin-9, claudin-19) containing K and D of opposite charge at the positions corresponding to K65 and S68 of claudin-17. Strikingly, all channel-forming classic claudins (claudin-2, claudin-10a, claudin-10b, claudin-15, and claudin-17) lack residues which electrostatically and sterically fit to each other at the corresponding positions. However, these positions could also contribute by other interactions to barrier versus channel formation. For instance, electrostatic networks to which residues corresponding not only to the claudin-17 positions 65 and 68 but also 57 and 63 were proposed to potentially contribute to *trans*-interactions which specifically tighten a gap between protomers for barrier-forming claudins such as claudin-1, claudin-3, and claudin-5 [57]. Further structure-function studies are needed to elucidate the molecular architecture of claudins-based paracellular ion channels within TJ strands.

Summary

The proximal tubule consists of a "leaky" epithelium which means that the paracellular pathway for ions is more permeable than the transcellular pathway. This causes transcellular reabsorption of ions and water to be boosted by paracellular passage. These functional features of the proximal tubule have been known for decades, but the molecular basis of paracellular ion and water transport was unknown then.

In "tight" epithelia, the paracellular pathway is predominantly sealed by numerous tight junction proteins of the claudin and the TAMP family. In the proximal tubule however, three claudins may be present which form paracellular channels (claudin-2, claudin-10a, and claudin-17) and only one sealing one (claudin-11).

Claudin-2 constitutes paracellular channels selective for small cations and by this contributes to reabsorption of Na^+ and K^+ in the proximal tubule. In contrast, here claudin-10a and perhaps also claudin-17 form channels selective for small anions which contribute to reabsorption of Cl^-. The pore of the claudin-2 channel is also permeable to water, resulting in 20–25% of proximal water absorption to take place paracellularly.

Ultrastructurally, the number of horizontal strands is one to two in the *pars convoluta* proximal tubules and three to five in *pars recta*. Nevertheless, the TJ seals the proximal tubule against back-leakage of larger solutes as nutrients.

Homology modeling of channel-forming claudins present in the proximal tubule proposes models that comprise *cis*-tetrameric units of claudin strands. On the surface of a cation- and an anion-selective claudin protomer differing electrostatic potentials are present in the area of the proposed ion channel, resulting in the opposite charge selectivity of these claudins.

Presently, the molecular structure of the claudin-based channels has only started to be fully understood.

References

1. Abuazza G, Becker A, Williams SS, Chakravarty S, Truong HT, Lin F, Baum M (2006) Claudins 6, 9, and 13 are developmentally expressed renal tight junction proteins. Am J Physiol Ren Physiol 291:F1132–F1141
2. Agre P, Preston GM, Smith BL, Jung JS, Raina S, Moon C, Guggino WB, Nielsen S (1993) Aquaporin CHIP: the archetypal molecular water channel. Am J Phys 265:F463–F476
3. Amasheh S, Meiri N, Gitter AH, Schöneberg T, Mankertz J, Schulzke JD, Fromm M (2002) Claudin-2 expression induces cation-selective channels in tight junctions of epithelial cells. J Cell Sci 115:4969–4976
4. Anderson JM, Van Itallie CM, Fanning AS (2004) Setting up a selective barrier at the apical junction complex. Curr Opin Cell Biol 16:140–145
5. Angelow S, Yu AS (2009) Structure-function studies of claudin extracellular domains by cysteine-scanning mutagenesis. J Biol Chem 284:29205–29217
6. Aronson PS, Giebisch G (1997) Mechanisms of chloride transport in the proximal tubule. Am J Phys 273:F179–F192
7. Barratt LJ, Rector FC Jr, Kokko JP, Seldin DW (1974) Factors governing the transepithelial potential difference across the proximal tubule of the rat kidney. J Clin Invest 53:454–464
8. Boulpaep EL (1971) Electrophysiological properties of the proximal tubule: importance of cellular and intercellular transport pathways. In: Giebisch G (ed) Electrophysiology of epithelial cells. Schattauer Verlag, Stuttgart, pp 98–112
9. Brandner JM, McIntyre M, Kief S, Wladykowski E, Moll I (2003) Expression and localization of tight junction-associated proteins in human hair follicles. Arch Dermatol Res 295:211–221
10. Branton D, Bullivant S, Gilula NB, Karnovsky MJ, Moor H, Mühlethaler K, Northcote DH, Packer L, Satir B, Satir P, Speth V, Staehlin LA, Steere RL, Weinstein RS (1975) Freeze-etching nomenclature. Science (New York, NY) 190:54–56
11. Cheval L, Pierrat F, Dossat C, Genete M, Imbert-Teboul M, Duong Van Huyen J-P, Poulain J, Wincker P, Weissenbach J, Piquemal D, Doucet A (2011) Atlas of gene expression in the mouse kidney: new features of glomerular parietal cells. Physiol Genomics 43:161–173
12. Claude P (1978) Morphological factors influencing transepithelial permeability: a model for the resistance of the *Zonula Occludens*. J Membr Biol 39:219–232
13. Claude P, Goodenough DA (1973) Fracture faces of zonulae occludentes from "tight" and "leaky" epithelia. J Cell Biol 58:390–400
14. Conrad MP, Piontek J, Günzel D, Fromm M, Krug SM (2016) Molecular basis of claudin-17 anion selectivity. Cell Mol Life Sci 73:185–200
15. Diamond JM (1978) Channels in epithelial cell membranes and junctions. Fed Proc 37:2639–2643

16. Diamond JM (1974) Tight and leaky junctions of epithelia: a perspective on kisses in the dark. Fed Proc 33:2220–2224
17. Duarte CG, Watson JF (1967) Calcium reabsorption in proximal tubule of the dog nephron. Am J Phys 212:1355–1360
18. Eichner M, Protze J, Piontek A, Krause G, Piontek J (2017) Targeting and alteration of tight junctions by bacteria and their virulence factors such as *Clostridium perfringens* enterotoxin. Pflügers Arch Eur J Physiol 469:77–90
19. Elkouby-Naor L, Abassi Z, Lagziel A, Gow A, Ben-Yosef T (2008) Double gene deletion reveals lack of cooperation between claudin 11 and claudin 14 tight junction proteins. Cell Tissue Res 333:427–438
20. Enck AH, Berger UV, Yu AS (2001) Claudin-2 is selectively expressed in proximal nephron in mouse kidney. Am J Physiol Ren Physiol 281:966–974
21. Farquhar MG, Palade GE (1963) Junctional complexes in various epithelia. J Cell Biol 17:375–412
22. France MM, Turner JR (2017) The mucosal barrier at a glance. J Cell Sci 130:307–314
23. Fujita H, Sugimoto K, Inatomi S, Maeda T, Osanai M, Uchiyama Y, Yamamoto Y, Wada T, Kojima T, Yokozaki H, Yamashita T, Kato S, Sawada N, Chiba H (2008) Tight junction proteins claudin-2 and -12 are critical for vitamin D-dependent Ca^{2+} absorption between enterocytes. Mol Biol Cell 19:1912–1921
24. Furuse M, Fujita K, Hiiragi T, Fujimoto K, Tsukita S (1998) Claudin-1 and -2: novel integral membrane proteins localizing at tight junctions with no sequence similarity to occludin. J Cell Biol 141:1539–1550
25. Furuse M, Furuse K, Sasaki H, Tsukita S (2001) Conversion of zonulae occludentes from tight to leaky strand type by introducing claudin-2 into Madin-Darby canine kidney I cells. J Cell Biol 153:263–272
26. Furuse M, Hirase T, Itoh M, Nagafuchi A, Yonemura S, Tsukita S, Tsukita S (1993) Occludin: a novel integral membrane protein localizing at tight junctions. J Cell Biol 123:1777–1788
27. Furuse M, Sasaki H, Tsukita S (1999) Manner of interaction of heterogeneous claudin species within and between tight junction strands. J Cell Biol 147:891–903
28. Gong Y, Renigunta V, Zhou Y, Sunq A, Wang J, Yang J, Renigunta A, Baker LA, Hou J (2015) Biochemical and biophysical analyses of tight junction permeability made of claudin-16 and claudin-19 dimerization. Mol Biol Cell 26:4333–4346
29. Günzel D, Fromm M (2012) Claudins and other tight junction proteins. Compr Physiol 2:1819–1852
30. Günzel D, Stuiver M, Kausalya PJ, Haisch L, Krug SM, Rosenthal R, Meij IC, Hunziker W, Fromm M, Müller D (2009) Claudin-10 exists in six alternatively spliced isoforms that exhibit distinct localization and function. J Cell Sci 122:1507–1517
31. Günzel D, Yu AS (2013) Claudins and the modulation of tight junction permeability. Physiol Rev 93:525–569
32. Guo P, Weinstein AM, Weinbaum S (2003) A dual-pathway ultrastructural model for the tight junction of rat proximal tubule epithelium. Am J Physiol Ren Physiol 285:F241–F257
33. Haddad M, Lin F, Dwarakanath V, Cordes K, Baum M (2005) Developmental changes in proximal tubule tight junction proteins. Pediatr Res 57:453–457
34. Ikenouchi J, Furuse M, Furuse K, Sasaki H, Tsukita S, Tsukita S (2005) Tricellulin constitutes a novel barrier at tricellular contacts of epithelial cells. J Cell Biol 171:939–945
35. Irudayanathan FJ, Trasatti JP, Karande P, Nangia S (2016) Molecular architecture of the blood brain barrier tight junction proteins—a synergistic computational and in vitro approach. J Phys Chem B 120:77–88
36. Kirk A, Campbell S, Bass P, Mason J, Collins J (2010) Differential expression of claudin tight junction proteins in the human cortical nephron. Nephrol Dial Transplant 25:2107–2119

37. Kiuchi-Saishin Y, Gotoh S, Furuse M, Takasuga A, Tano Y, Tsukita S (2002) Differential expression patterns of claudins, tight junction membrane proteins, in mouse nephron segments. J Am Soc Nephrol 13:875–886
38. Krause G, Protze J, Piontek J (2015) Assembly and function of claudins: structure-function relationships based on homology models and crystal structures. Semin Cell Dev Biol 42:3–12
39. Krug SM (2017) Contribution of the tricellular tight junction to paracellular permeability in leaky and tight epithelia. Ann N Y Acad Sci doi:10.1111/nyas.13379 (in press)
40. Krug SM, Amasheh M, Dittmann I, Christoffel I, Fromm M, Amasheh S (2013) Sodium caprate as an enhancer of macromolecule permeation across tricellular tight junctions of intestinal cells. Biomaterials 34:275–282
41. Krug SM, Amasheh S, Richter JF, Milatz S, Günzel D, Westphal JK, Huber O, Schulzke JD, Fromm M (2009) Tricellulin forms a barrier to macromolecules in tricellular tight junctions without affecting ion permeability. Mol Biol Cell 20:3713–3724
42. Krug SM, Günzel D, Conrad MP, Rosenthal R, Fromm A, Amasheh S, Schulzke JD, Fromm M (2012) Claudin-17 forms tight junction channels with distinct anion selectivity. Cell Mol Life Sci 69:2765–2778
43. Krug SM, Schulzke JD, Fromm M (2014) Tight junction, selective permeability, and related diseases. Semin Cell Dev Biol 36:166–176
44. Li J, Zhuo M, Pei L, Rajagopal M, Yu AS (2014) Comprehensive cysteine-scanning mutagenesis reveals Claudin-2 pore-lining residues with different intrapore locations. J Biol Chem 289:6475–6484
45. Liebner S, Kniesel U, Kalbacher H, Wolburg H (2000) Correlation of tight junction morphology with the expression of tight junction proteins in blood-brain barrier endothelial cells. Eur J Cell Biol 79:707–717
46. Marcial MA, Carlson SL, Madara JL (1984) Partitioning of paracellular conductance along the ileal crypt-villus axis: a hypothesis based on structural analysis with detailed consideration of tight junction structure-function relationships. J Membr Biol 80:59–70
47. Martinez-Palomo A, Erlij D (1975) Structure of tight junctions in epithelia with different permeability. Proc Natl Acad Sci U S A 72:4487–4491
48. Menco BP (1988) Tight-junctional strands first appear in regions where three cells meet in differentiating olfactory epithelium: a freeze-fracture study. J Cell Sci 89(Pt 4):495–505
49. Milatz S, Breiderhoff T (2017) One gene, two paracellular ion channels—claudin-10 in the kidney. Pflügers Arch Eur J Physiol 469:115–121
50. Milatz S, Himmerkus N, Wulfmeyer VC, Drewell H, Mutig K, Hou J, Breiderhoff T, Müller D, Fromm M, Bleich M, Günzel D (2017) Mosaic expression of claudins in thick ascending limbs of Henle results in spatial separation of paracellular Na+ and Mg2+ transport. Proc Natl Acad Sci U S A 114:E219–e227
51. Milatz S, Krug SM, Rosenthal R, Günzel D, Müller D, Schulzke JD, Amasheh S, Fromm M (2010) Claudin-3 acts as a sealing component of the tight junction for ions of either charge and uncharged solutes. Biochim Biophys Acta 1798:2048–2057
52. Milatz S, Piontek J, Hempel C, Grohe C, Fromm A, Lee IM, El-Athman R, Günzel D (2017) Tight junction strand formation by claudin-10 isoforms and claudin-10a/−10b chimeras. Ann N Y Acad Sci, doi:10.1111/nyas.13393 (in press)
53. Milatz S, Piontek J, Schulzke JD, Blasig IE, Fromm M, Günzel D (2015) Probing the cis-arrangement of prototype tight junction proteins claudin-1 and claudin-3. Biochem J 468:449–458
54. Morita K, Furuse M, Fujimoto K, Tsukita S (1999) Claudin multigene family encoding four-transmembrane domain protein components of tight junction strands. Proc Natl Acad Sci U S A 96:511–516

55. Muto S, Hata M, Taniguchi J, Tsuruoka S, Moriwaki K, Saitou M, Furuse K, Sasaki H, Fujimura A, Imai M, Kusano E, Tsukita S, Furuse M (2010) Claudin-2-deficient mice are defective in the leaky and cation-selective paracellular permeability properties of renal proximal tubules. Proc Natl Acad Sci U S A 107:8011–8016

56. Pei L, Solis G, Nguyen MT, Kamat N, Magenheimer L, Zhuo M, Li J, Curry J, McDonough AA, Fields TA, Welch WJ, Yu AS (2016) Paracellular epithelial sodium transport maximizes energy efficiency in the kidney. J Clin Invest 126:2509–2518

57. Piontek A, Rossa J, Protze J, Wolburg H, Hempel C, Günzel D, Krause G, Piontek J (2017) Polar and charged extracellular residues conserved among barrier-forming claudins contribute to tight junction strand formation. Ann N Y Acad Sci, doi:10.1111/nyas.13341 (in press)

58. Piontek J, Fritzsche S, Cording J, Richter S, Hartwig J, Walter M, Yu D, Turner JR, Gehring C, Rahn HP, Wolburg H, Blasig IE (2011) Elucidating the principles of the molecular organization of heteropolymeric tight junction strands. Cell Mol Life Sci 68:3903–3918

59. Piontek J, Winkler L, Wolburg H, Müller SL, Zuleger N, Piehl C, Wiesner B, Krause G, Blasig IE (2008) Formation of tight junction: determinants of homophilic interaction between classic claudins. FASEB J 22:146–158

60. Pricam C, Fisher KA, Friend DS (1977) Intramembranous particle distribution in human erythrocytes: effects of lysis, glutaraldehyde, and poly-L-lysine. Anat Rec 189:595–607

61. Protze J, Eichner M, Piontek A, Dinter S, Rossa J, Blecharz KG, Vajkoczy P, Piontek J, Krause G (2015) Directed structural modification of Clostridium perfringens enterotoxin to enhance binding to claudin-5. Cell Mol Life Sci 72:1417–1432

62. Roesinger B, Schiller A, Taugner R (1978) A freeze-fracture study of tight junctions in the pars convoluta and pars recta of the renal proximal tubule. Cell Tissue Res 186:121–133

63. Rosenthal R, Günzel D, Krug SM, Schulzke JD, Fromm M, Yu AS (2017) Claudin-2-mediated cation and water transport share a common pore. Acta Physiol (Oxford, England) 219:521–536

64. Rosenthal R, Milatz S, Krug SM, Oelrich B, Schulzke JD, Amasheh S, Günzel D, Fromm M (2010) Claudin-2, a component of the tight junction, forms a paracellular water channel. J Cell Sci 123:1913–1921

65. Rossa J, Ploeger C, Vorreiter F, Saleh T, Protze J, Günzel D, Wolburg H, Krause G, Piontek J (2014) Claudin-3 and claudin-5 protein folding and assembly into the tight junction are controlled by non-conserved residues in the transmembrane 3 (TM3) and extracellular loop 2 (ECL2) segments. J Biol Chem 289:7641–7653

66. Rossa J, Protze J, Kern C, Piontek A, Günzel D, Krause G, Piontek J (2014) Molecular and structural transmembrane determinants critical for embedding claudin-5 into tight junctions reveal a distinct four-helix bundle arrangement. Biochem J 464:49–60

67. Saitoh Y, Suzuki H, Tani K, Nishikawa K, Irie K, Ogura Y, Tamura A, Tsukita S, Fujiyoshi Y (2015) Tight junctions. Structural insight into tight junction disassembly by Clostridium perfringens enterotoxin. Science (New York, NY) 347:775–778

68. Schiller A, Tiedemann K (1981) The mature mesonephric nephron of the rabbit embryo. III. Freeze-fracture studies. Cell Tissue Res 221:431–442

69. Schnermann J, Chou CL, Ma T, Traynor T, Knepper MA, Verkman AS (1998) Defective proximal tubular fluid reabsorption in transgenic aquaporin-1 null mice. Proc Natl Acad Sci U S A 95:9660–9664

70. Schnermann J, Huang Y, Mizel D (2013) Fluid reabsorption in proximal convoluted tubules of mice with gene deletions of claudin-2 and/or aquaporin1. Am J Physiol Ren Physiol 305:F1352–F1364

71. Seldin DW (1999) Renal handling of calcium. Nephron 81(Suppl 1):2–7

72. Shen L, Weber CR, Raleigh DR, Yu D, Turner JR (2011) Tight junction pore and leak pathways: a dynamic duo. Annu Rev Physiol 73:283–309

73. Shinoda T, Shinya N, Ito K, Ohsawa N, Terada T, Hirata K, Kawano Y, Yamamoto M, Kimura-Someya T, Yokoyama S, Shirouzu M (2016) Structural basis for disruption of claudin assembly in tight junctions by an enterotoxin. Sci Rep 6:33632

74. Staehelin LA (1973) Further observations on the fine structure of freeze-cleaved tight junctions. J Cell Sci 13:763–786

75. Staehelin LA (1974) Structure and function of intercellular junctions. Int Rev Cytol 39:191–283

76. Staehelin LA, Mukherjee TM, Williams AW (1969) Freeze-etch appearance of the tight junctions in the epithelium of small and large intestine of mice. Protoplasma 67:165–184

77. Steed E, Rodrigues NT, Balda MS, Matter K (2009) Identification of MarvelD3 as a tight junction-associated transmembrane protein of the occludin family. BMC Cell Biol 10:95

78. Suzuki H, Nishizawa T, Tani K, Yamazaki Y, Tamura A, Ishitani R, Dohmae N, Tsukita S, Nureki O, Fujiyoshi Y (2014) Crystal structure of a claudin provides insight into the architecture of tight junctions. Science (New York, NY) 344:304–307

79. Suzuki H, Tani K, Tamura A, Tsukita S, Fujiyoshi Y (2015) Model for the architecture of claudin-based paracellular ion channels through tight junctions. J Mol Biol 427:291–297

80. Tőkés A-M, Szász AM, Juhász É, Schaff Z, Harsányi L, Molnár IA, Baranyai Z, Besznyák I, Zaránd A, Salamon F, Kulka J (2012) Expression of tight junction molecules in breast carcinomas analysed by array PCR and immunohistochemistry. Pathol Oncol Res 18:593–606

81. Van Itallie C, Rahner C, Anderson JM (2001) Regulated expression of claudin-4 decreases paracellular conductance through a selective decrease in sodium permeability. J Clin Invest 107:1319–1327

82. Van Itallie CM, Holmes J, Bridges A, Gookin JL, Coccaro MR, Proctor W, Colegio OR, Anderson JM (2008) The density of small tight junction pores varies among cell types and is increased by expression of claudin-2. J Cell Sci 121:298–305

83. Van Itallie CM, Rogan S, Yu A, Vidal LS, Holmes J, Anderson JM (2006) Two splice variants of claudin-10 in the kidney create paracellular pores with different ion selectivities. Am J Physiol Ren Physiol 291:F1288–F1299

84. Wada M, Tamura A, Takahashi N, Tsukita S (2013) Loss of claudins 2 and 15 from mice causes defects in paracellular Na^+ flow and nutrient transport in gut and leads to death from malnutrition. Gastroenterology 144:369–380

85. Watson CJ, Rowland M, Warhurst G (2001) Functional modeling of tight junctions in intestinal cell monolayers using polyethylene glycol oligomers. Am J Phys Cell Phys 281:C388–C397

86. Wolburg H, Neuhaus J, Kniesel U, Krauss B, Schmid EM, Ocalan M, Farrell C, Risau W (1994) Modulation of tight junction structure in blood-brain barrier endothelial cells. Effects of tissue culture, second messengers and cocultured astrocytes. J Cell Sci 107(Pt 5):1347–1357

87. Yu AS, Cheng MH, Angelow S, Günzel D, Kanzawa SA, Schneeberger EE, Fromm M, Coalson RD (2009) Molecular basis for cation selectivity in claudin-2-based paracellular pores: identification of an electrostatic interaction site. J Gen Physiol 133:111–127